The phosphoinositide-associated protein Rush hour regulates endosomal trafficking in *Drosophila*

Ieva Gailite, Diane Egger-Adam, and Andreas Wodarz
Stammzellbiologie, Abteilung Anatomie und Zellbiologie, Georg-August-Universität Göttingen, 37077 Göttingen, Germany

ABSTRACT Endocytosis regulates multiple cellular processes, including the protein composition of the plasma membrane, intercellular signaling, and cell polarity. We have identified the highly conserved protein Rush hour (Rush) and show that it participates in the regulation of endocytosis. Rush localizes to endosomes via direct binding of its FYVE (Fab1p, YOTB, Vac1p, EEA1) domain to phosphatidylinositol 3-phosphate. Rush also directly binds to Rab GDP dissociation inhibitor (Gdi), which is involved in the activation of Rab proteins. Homozygous *rush* mutant flies are viable but show genetic interactions with mutations in *Gdi*, *Rab5*, *hrs*, and *carnation*, the fly homologue of Vps33. Overexpression of Rush disrupts progression of endocytosed cargo and increases late endosome size. Lysosomal marker staining is decreased in Rush-overexpressing cells, pointing to a defect in the transition between late endosomes and lysosomes. Rush also causes formation of endosome clusters, possibly by affecting fusion of endosomes via an interaction with the class C Vps/homotypic fusion and vacuole protein-sorting (HOPS) complex. These results indicate that Rush controls trafficking from early to late endosomes and from late endosomes to lysosomes by modulating the activity of Rab proteins.

INTRODUCTION

In eukaryotic cells endocytosis regulates the exchange of molecules both between the cell and its environment and between intracellular organelles. Molecules that are taken up from the plasma membrane are delivered to early endosomes and subsequently either travel to lysosomes via late endosomes or are returned to the plasma membrane via recycling endosomes. The identity of endosomal compartments is ensured by specific localization of highly regulated proteins,

for example Rab guanosine triphosphatases (GTPases; Zerial and McBride, 2001). Rabs regulate vesicle budding, transport, and fusion (Zerial and McBride, 2001; Grosshans *et al.*, 2006). After being endocytosed from the plasma membrane, Rab5 regulates early endosome formation and homotypic fusion (Gorvel *et al.*, 1991; Bucci *et al.*, 1992; Morrison *et al.*, 2008). In the transition between early and late endosomes, Rab5 is replaced by Rab7 (Rink *et al.*, 2005), which is necessary for late endosome function (Feng *et al.*, 1995; Vitelli *et al.*, 1997; Vanlandingham and Ceresa, 2009). The transition between early and late endosome identity has been proposed to take place via interaction of active Rab5 with Rab7 guanine nucleotide exchange factor (GEF), thus leading to the activation of Rab7. The identity of Rab7 GEF has been under discussion, attributing this role to either Vps39 (Wurmser *et al.*, 2000) or, more recently, the Mon1/Ccz1 complex (Kinchen and Ravichandran, 2010; Nordmann *et al.*, 2010; Poteryaev *et al.*, 2010). Regardless of its disputable role as Rab7 GEF, Vps39 has been described as being required for the transition from early to late endosome (Ostrowicz *et al.*, 2010; Poteryaev *et al.*, 2010). Vps39 is a part of the class C Vps/homotypic fusion and vacuole protein sorting (Vps/HOPS) complex, which consists of six subunits—the core formed by Vps11, Vps16, Vps18 (Dor in *Drosophila*), Vps33 (Car), and two additional subunits, Vps39 and Vps41. The HOPS complex plays multiple roles in endosome

Abbreviations used: *arm*, *armadillo*; Avl, Avalanche; *car*, *carnation*; CORVET complex class C core vacuole/endosome-tethering complex; *dor*, *deep orange*; FRET, fluorescence resonance energy transfer; GDI, GDP dissociation inhibitor; GDP, guanosine diphosphate; GEF, guanine nucleotide exchange factor; GFP, green fluorescent protein; GTPase, guanosine triphosphatase; HOPS complex, homotypic fusion and vacuole protein-sorting complex; MBP, maltose-binding protein; PBS, phosphate-buffered saline; PIP, phosphatidylinositol phosphates; PI(3)P, phosphatidylinositol 3-phosphate; PNS, postnuclear supernatant; Rush, Rush hour; TBS, Tris-buffered saline; TNF, tumor necrosis factor; UTR, untranslated region; YFP, yellow fluorescent protein.

trafficking, including tethering and fusion of late endosomes and lysosomes (Wurmser et al., 2000; Akbar et al., 2009; Hickey and Wickner, 2010; Pieren et al., 2010), lysosome biogenesis (Sevrioukov et al., 1999; Sriram et al., 2003), and endosome maturation (Rink et al., 2005; Chotard et al., 2010). The core subunits of the HOPS complex, together with two associated proteins, Vps3 and Vps8, that replace Vps39 and Vps41, also participate in formation of the class C core vacuole/endosome-tethering (CORVET) complex (Peplowska et al., 2007). This complex has functions similar to the HOPS complex but acts on early and/or late endosome tethering (Peplowska et al., 2007; Markgraf et al., 2009).

Activity of Rabs is regulated by their GTPase cycle. After GTP hydrolysis, inactive guanosine diphosphate (GDP)-bound Rab is removed from the membrane by binding to a GDP dissociation inhibitor (GDI). Inactive Rab can then be delivered back to the donor compartment and converted to an active state by a GEF that catalyzes exchange of GDP to GTP. GDI acts as a negative regulator of Rab activity, and has been shown to inhibit the fusion of late endosomes with lysosomes (Mullock et al., 1998). While the function of GDI in recycling of Rabs has been investigated in detail, not much is known about regulation of GDI itself (Cavalli et al., 2001). A single GDI homologue exists in flies (Ricard et al., 2001), but its function has not been well characterized.

In this work, we characterize a novel endosomal protein, which we named Rush hour (Rush) due to its overexpression phenotype. Rush shows high sequence similarity along its entire length with homologues in other organisms from *Caenorhabditis elegans* to vertebrates (74.6% sequence identity between *Drosophila melanogaster* and *Homo sapiens*). Rush contains two phosphoinositide-binding domains, a PH (pleckstrin homology) domain and a FYVE (Fab1p, YOTB, Vac1p, EEA1) domain. Most FYVE domain–containing proteins localize to endosomes (Gillooly et al., 2001), suggesting that Rush might be involved in endocytosis. Rush has two human homologues, Phafin1 and Phafin2, which have been described as regulating Rab5-mediated endocytosis (Lin et al., 2010) and participating in tumor necrosis factor (TNF)-dependent apoptosis (Chen et al., 2005; Li et al., 2008; Lin et al., 2010). Interestingly, Phafin2 is overexpressed in several cancer types, including human hepatocellular carcinoma and breast cancer (Chen et al., 2002; Weisz et al., 2004; Lin et al., 2010). In this study, we demonstrate that Rush is associated with endosomal membranes and regulates endosomal trafficking. Rush binds GDI and recruits GDI to endosomal membranes. These biochemical and immunohistochemical data are complemented by data on genetic interactions between *rush*, *Rab5*, *Gdi*, *hrs*, and *car*, together pointing to a function of Rush in regulation of Rab activity.

RESULTS

Rush localizes to endosomes

To analyze the subcellular localization of Rush, we generated an antibody against a peptide corresponding to its N-terminus. Immunofluorescence stainings of wild-type ovaries showed that Rush is expressed both in the germ line and in the overlying somatic follicular epithelium (Figure 1A). In the follicular epithelium, Rush localized to the lateral cell cortex with lesser amounts of the protein present at the apical membrane (Figure 1B). Interestingly, Rush colocalized with Hrs in the oocyte of stage 8 egg chambers in prominent subcellular structures (Figure 1A, arrowhead; Januschke et al., 2007; Tanaka and Nakamura, 2008). Hrs is a FYVE domain–containing protein that regulates the transition between early and late endosomes (Lloyd et al., 2002). To investigate the potential association of Rush with endosomes, we analyzed colocalization of Rush with markers of different endosomal compartments in the follicular epithelium (Figure 1, C–G;

quantification in Figure 1H and Supplemental Figure S2G). Rush colocalized with Avalanche (Avl), a syntaxin that regulates early endocytotic steps (Figure 1C; Lu and Bilder, 2005), Hrs (Figure 1D), the early endosome marker YFP-Rab5 (Figure 1E), and the late endosome marker YFP-Rab7 (Figure 1F). Less colocalization was observed with the marker of recycling endosomes YFP-Rab11 (Figure 1G). To further test the association of Rush with endosomes, we separated endosomal fractions from S2 cell lysates via sucrose gradient ultracentrifugation (Figure 1I). Rush was detected in fraction 1, together with Rab5 and Rab7, but not in fraction 2 that contained Rab7 alone. Rush was localized in a wild-type manner in *hrs*[D28] follicular cell clones (Figure S1), indicating that Rush becomes associated with endosomes before formation of multivesicular bodies (Lloyd et al., 2002). Therefore Rush seems to associate both with early and late endosomes.

To further analyze the association of Rush with endosomes, we generated a C-terminal Rush-green fluorescent protein (GFP)-fusion protein. When overexpressed in the follicular epithelium under the control of *Cu1::GAL4*, Rush-GFP localized to the lateral cortex and to endosomes (Figure S2, A–E) in a manner similar to the endogenous protein (Figure 1). Like endogenous Rush, Rush-GFP showed significant colocalization with Avl, Hrs, and Rab7 (Figure S2, A, C, and D), but less colocalization with Rab11 (Figure S2E; quantification shown in Figure S2F). Interestingly, overexpression of Rush-GFP increased colocalization between Rush and Rab7 on endosomes from R = 0.41 (Figure S2G) to R = 0.75 (Figure S2F; p = 0.0001), demonstrating that the amount of Rab7 recruited to Rush-positive endosomes was strongly increased upon Rush-GFP overexpression. Since colocalization of Avl and Rab7 in endosomal compartments in wild type is not observed (Lu and Bilder, 2005), Rush overexpression might induce the formation of a hybrid compartment with characteristics of early and late endosomes. Rush-GFP–positive endosomes contained endocytosed Notch and E-cadherin, demonstrating that Rush overexpression does not impair endocytosis of transmembrane proteins from the plasma membrane (Figure S3).

Rush interacts with phosphoinositides via its lipid-binding domains

Since Rush localizes both to the plasma membrane and endosomes, the two lipid-binding domains of Rush, a PH and a FYVE domain (Figures 2B and S4), could mediate its membrane association. Both FYVE and PH domains interact with but differ in their affinity for phosphatidylinositol phosphates (PIPs). FYVE domains have been described as binding specifically to phosphatidylinositol 3-phosphate (PI(3)P), a phosphoinositide found on early endosomes and multivesicular bodies (Gillooly et al., 2001; van Meer et al., 2008), while PH domains interact with a broader range of PIPs (Currie et al., 1999; Dowler et al., 2000; Varnai et al., 2002). Therefore our aim was to determine the lipid-binding affinity of Rush. For this purpose, we performed lipid overlay assays with glutathione S-transferase (GST)-tagged full-length Rush and its separate domains. GST-fusion proteins were incubated with phospholipids immobilized on a nitrocellulose membrane (PIP Strips; Figure 2A). The PH domain of Rush interacted most strongly with PI(3,4)P_2 and PI(4)P and had a weaker interaction with PI(3)P. The FYVE domain, as expected, interacted exclusively with PI(3)P. Full-length Rush interacted most strongly with PI(3)P, but also bound to a lesser extent to PI(4)P, PI(5)P, PI(3,4)P_2, PI(4,5)P_2, and PI(3,4,5)P_3 (Figure 2A). Thus the lipid-binding domains of Rush are able to interact with PIPs, and Rush has the highest affinity toward PI(3)P, a lipid specific for early endosomes and multivesicular bodies. Therefore both predicted lipid-interacting domains of Rush are able to bind to phosphoinositides and could target Rush to membranes.
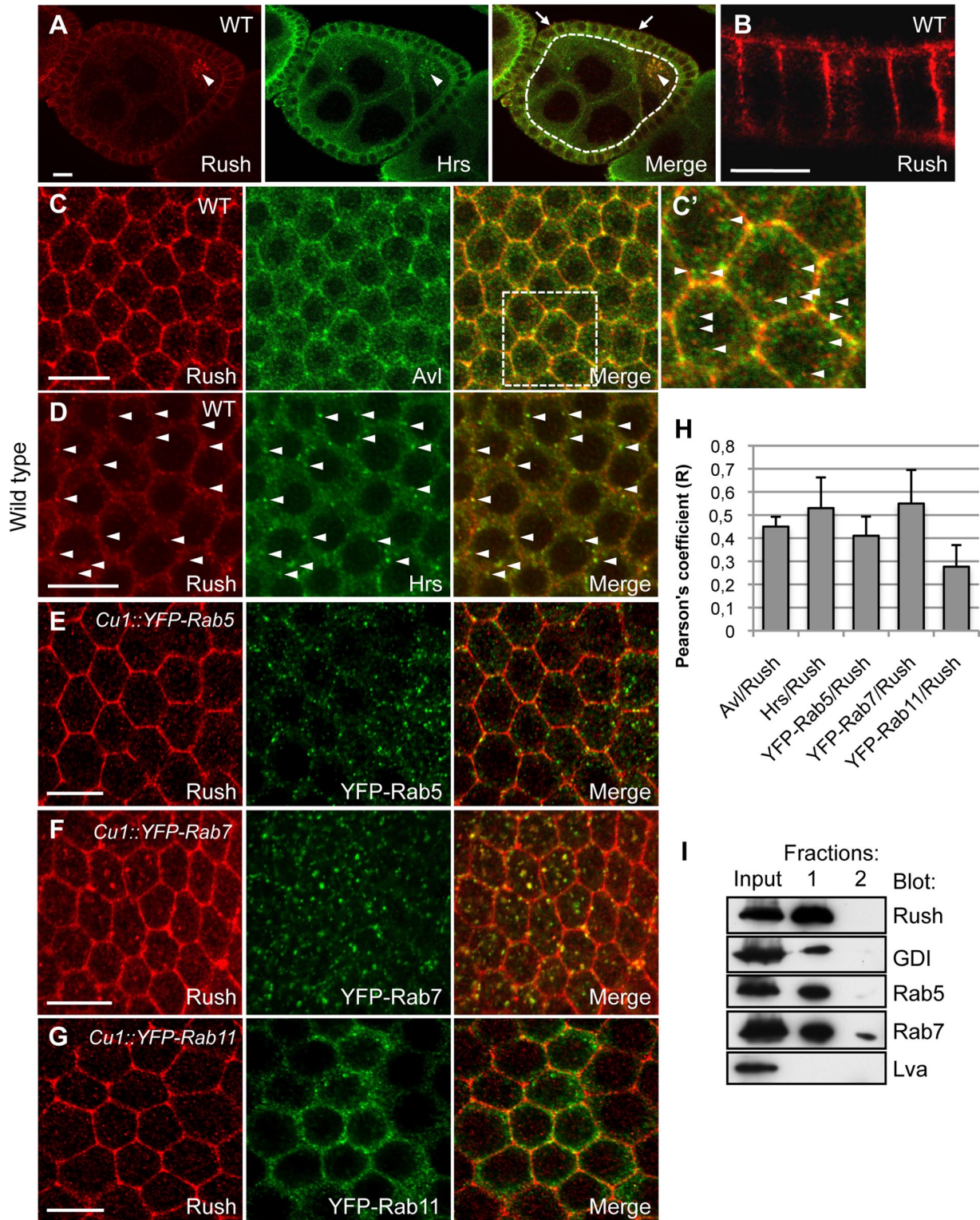
FIGURE 1: Rush localizes to endosomes. (A) Rush is expressed both in germ line cells (encircled by dotted line in merged image) and in the follicular epithelium (arrows). Rush colocalizes with Hrs in the oocyte (arrowhead). (B) Rush accumulates at the lateral plasma membrane in the follicular cell epithelium. (C–G). Colocalization of Rush and different endosomal markers in the follicular epithelium. C′ is a magnification of the marked region in C. (H) Colocalization was quantified using ImageJ Colocalization Threshold plug-in, which produced Pearson's correlation coefficient (R). Pearson's coefficient represents intensity correlation of all non-zero-zero pixels that overlay in images of two channels. Error bars show SD. (I) Rush cofractionates with GDI, Rab5, and Rab7. Untransfected S2 cell lysates were subjected to discontinuous sucrose gradient ultracentrifugation to separate fractions enriched in early endosomes (1) and late endosomes (2). Rush sediments in fraction 1, which contains both Rab5 and Rab7. The Golgi marker Lava lamp (Lva) was used as negative control for the fractionation. (A–G) Genotypes are given at the top of each panel. wt, wild type. Anterior is to the left. Scale bars: 10 μm.
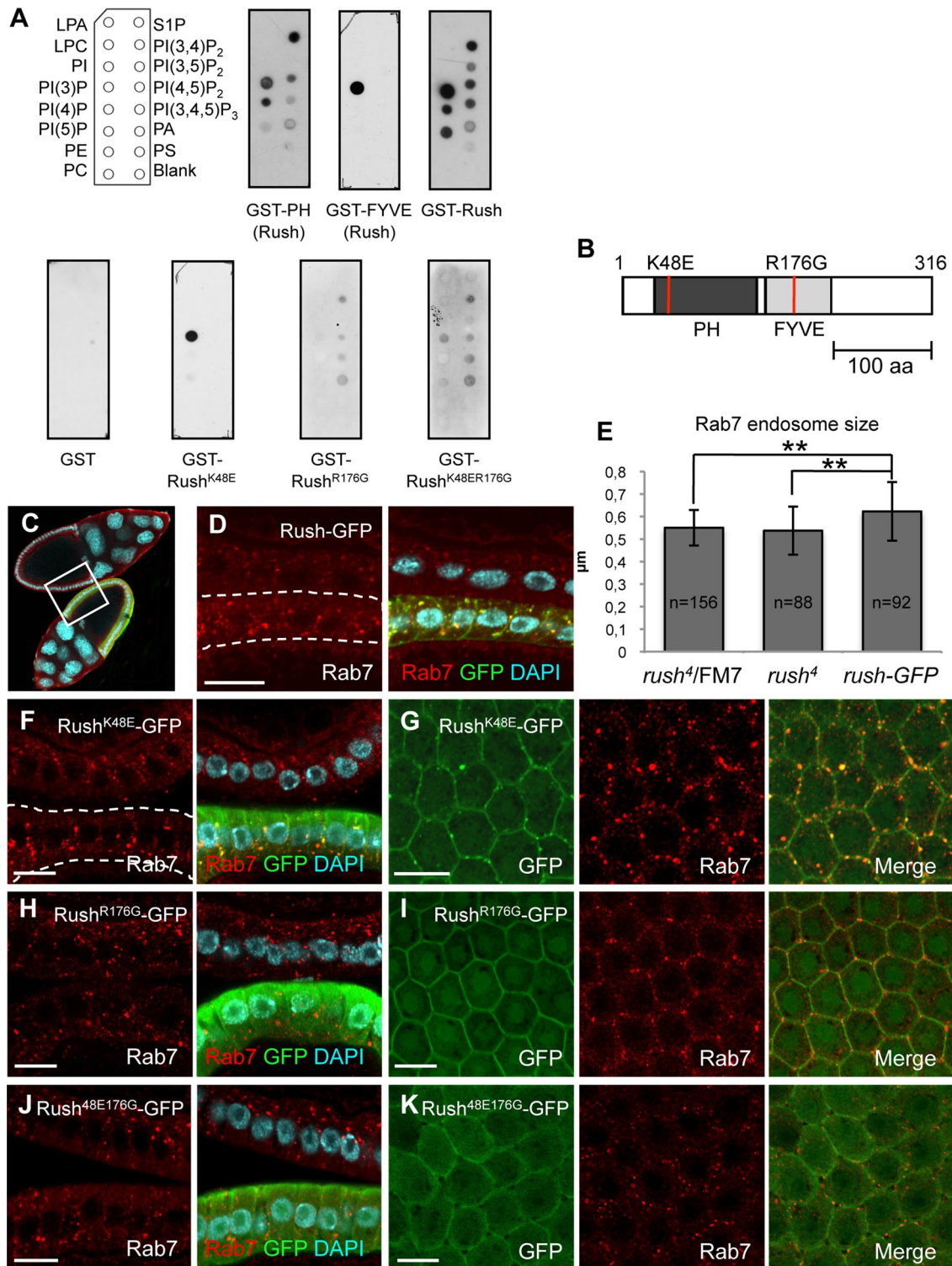
FIGURE 2: Rush lipid-binding domains interact with phosphoinositides and regulate intracellular localization of Rush. (A) Phospholipid binding of Rush was detected by incubating PIP Strips with GST-fusion proteins of Rush PH and FYVE domains alone or full-length GST-Rush. GST was used as a negative control. (B) Scheme of the Rush protein, showing the position of amino acid exchanges (red bars) that abolish lipid binding of PH and FYVE domains. (C) Rab7 vesicle size was compared in follicular epithelia of two adjacent egg chambers at the same developmental stage, one of which expresses Rush-GFP driven by the Cu1::GAL4 driver, while the other one expresses Cu1::GAL4 only. The marked area represents an area like the ones shown in (D), (F), (H), and (J). (D) Overexpression of Rush-GFP under the control of Cu1::GAL4 leads to accumulation of enlarged Rab7-positive endosomes. (E) Quantification of Rab7-positive endosome size in follicular epithelium of different genotypes. Error bars indicate SEM. ** $p < 0.01$. (F and G) Rush[K48E]-GFP localizes to the plasma membrane and Rab7-positive endosomes and causes increased late endosome size. Rush[R176G]-GFP (H and I) and Rush[K48ER176G]-GFP (J and K) do not localize to endosomes and are present at the plasma membrane and in the cytosol. Scale bars: 10 μm.

Localization of Rush to endosomes requires a functional FYVE domain

To analyze how the PH and FYVE domains affect the subcellular localization of Rush, our aim was to eliminate lipid-binding properties of each of the domains. Single amino acid exchange mutations that abolish lipid binding of PH and FYVE domains have been described (Yagisawa *et al.*, 1998; Kutateladze, 2006). In both domains, basic amino acid residues are responsible for the interaction with phospholipids. In the FYVE domain, the core motif RR/KHHCR is responsible for the interaction of the domain with PI(3)P. Mutations in any of the arginine or histidine residues in this motif lead to disruption of the lipid binding (Gaullier *et al.*, 2000). On the basis of these findings, we exchanged the Arg-176 residue of Rush with glycine using site-directed mutagenesis, which resulted in a complete loss of the binding to PI(3)P, as expected (Figure 2A). Exchange of Lys-32 for glutamic acid in the phospholipase Cγ PH domain abolished the ability of the protein to interact with P(4,5)P_2 (Yagisawa *et al.*, 1998). The homologous residue Lys-48 in the PH domain of Rush was mutated to glutamic acid, resulting in the loss of binding to PIPs (Figure 2, A and B). The full-length Rush[K48E] interacted only with PI(3)P due to the activity of the FYVE domain. Rush[K48ER176G] was not able to bind PIPs and exhibited only background interaction levels. Interestingly, Rush[R176G] also lost its affinity to PIPs, although one would expect a similar affinity to PIPs as in the case of the PH domain alone (Figure 2A). This effect might be caused by conformational changes in the protein caused by the mutation. It is also possible that activity of both PH and FYVE domains in a full-length protein is necessary for lipid association of Rush.

To observe how the mutations in lipid-binding domains affect the localization of Rush in cells, transgenic flies expressing mutated, full-length Rush proteins tagged with GFP were created. When expressed in the follicular epithelium, Rush[K48E]-GFP could still localize to the cell cortex and endosomes, indicating that the FYVE domain of Rush is sufficient for membrane localization of Rush (Figure 2, F and G). Although the majority of FYVE domains analyzed so far localize exclusively to endosomes (Kutateladze, 2006), several FYVE domains have been reported to localize to the plasma membrane (Kim *et al.*, 2002; Nagano *et al.*, 2010). To test the possibility that the FYVE domain of Rush mediates its localization at the plasma membrane, we expressed the GFP-tagged FYVE domain of Rush (FYVE[Rush]) in the follicular epithelium. The bulk of GFP-FYVE[Rush] localized to large particles that probably represent cortical endosomes (Figure S5F). However, a fraction of GFP-FYVE[Rush] was indeed found at the plasma membrane (Figure S5F). Thus the FYVE domain of Rush is the first FYVE domain described in *Drosophila* that mediates both endosome targeting and localization to the plasma membrane. Unexpectedly, Rush[R176G]-GFP was detected at the cell cortex (Figure 2, H and I), although no significant affinity of Rush[R176G] toward PIPs could be detected in the lipid overlay assay (Figure 2A). Rush[R176G]-GFP did not colocalize with cytoplasmic Rab7 puncta, indicating that the FYVE domain of Rush is needed for the association with endosomes (Figure 2, H and I). Rush[K48ER176G]-GFP, as expected from the lipid overlay assay, was distributed in the cytoplasm (Figure 2, J and K) and exhibited only weak association with the plasma membrane (Figure 2K), suggesting an additional interaction with an unknown plasma membrane protein might take place. When expressed in the *rush* mutant background, all three mutant Rush constructs maintained the same localization pattern as in the wild-type background, showing that a possible dimerization with endogenous Rush does not affect Rush localization (Figure S5, C–E).

Overexpression of endosome-associated Rush increases late endosome size

Overexpression of Rush-GFP in the follicular epithelium caused an increase in size of Rab7 endosomes in comparison with endosomes of the wild-type tissue (Figures 2, C–E, and S5A). Overexpression of untagged Rush in follicular cells also caused formation of larger Hrs-positive endosomes (Figure S5B). This effect depended on localization of Rush to endosomes, since Rush[K48E]-GFP also led to formation of large Rab7-positive endosomes (Figure 2F), while Rush[R176G]-GFP or Rush[K48ER176G]-GFP, which are unable to localize to endosomes, did not affect late endosome size (Figure 2, H and J).

Rush overexpression affects endocytic cargo progression

The increased endosome size in Rush-overexpressing cells indicated that trafficking from these endosomes to downstream compartments of the endocytic pathway might be affected. To analyze the progression of endocytic cargo, we overexpressed Rush-GFP in the posterior compartment of wing imaginal disks under control of en::GAL4 and followed the uptake and degradation of fluorescently labeled dextran (Figure 3, A–D). Endocytic uptake of dextran was normal in Rush-overexpressing cells and, after a 5-min chase, dextran colocalized with Rush-positive vesicles (Figure 3B). In wild-type cells marked by absence of GFP, levels of intracellular dextran decreased after 30- to 60-min chases, most probably due to lysosomal degradation (Figure 3, C and D). In contrast, dextran remained trapped in Rush-positive vesicles in Rush-overexpressing tissue (Figure 3, C and D). In addition, staining for LysoTracker, a dye that marks acidic cellular compartments, was slightly reduced in these cells (Figure 3, E and F). LysoTracker staining was also decreased in follicular cells that overexpressed Rush-GFP (Figure 3, G and H), but not upon overexpression of Rush[R176G]-GFP (Figure 3I), which is unable to localize to endosomes (Figure 2, H and I). Therefore the progression of endosomal cargo and acidification of lysosomes appears to be disrupted upon Rush overexpression.

rush is not required for fly viability

To further analyze the function of Rush, we generated a *rush* null allele via FLP recombinase/FLP recombinase target (FLP/FRT)–mediated excision (Parks *et al.*, 2004). The insertion points of transposons used to generate a deletion of the whole *rush* locus are depicted in Figure 4A. The P(XP)CG14782[d03799] element is located in the 5′ untranslated region (UTR) of *rush*, while the pBac(WH)f03712 element is inserted into the 5′ UTR of *sta*, a gene located downstream of *rush*. Consequently, the *sta* gene was also removed during the recombination (Figure 4A). *sta* is an essential gene, therefore a rescue construct containing the full-length coding sequence of *sta*, including the upstream regulatory sequences (Melnick *et al.*, 1993), was crossed in after the recombination to complement the loss of *sta* function. The *rush*[4] mutant flies obtained in this way were homozygous viable and fertile. To verify that the mutant line represents a *rush* null allele, we performed Western blot analysis on protein extracts from flies of the original transposon insertion lines and from the *rush*[4] mutant flies (Figure 4B). Western blotting with the antibody against the N-terminus of Rush resulted in a band of ~40 kDa that corresponds to full-length Rush in the extracts from the original transposon insertion stocks. In comparison, no signal for Rush was detected in the *rush*[4] embryo extract, indicating that *rush*[4] is indeed a null allele. Additionally, no immunofluorescence signal for Rush could be detected in *rush*[4] follicular epithelium in comparison with the wild type (Figure 4, C–F). Homozygous mutant *rush*[4] cells did not show alterations in the subcellular localization or amount of Rab7 (Figure 4, G and H), Rab11 (Figure 4, I and J), and Avl (Figure 4, K and L).
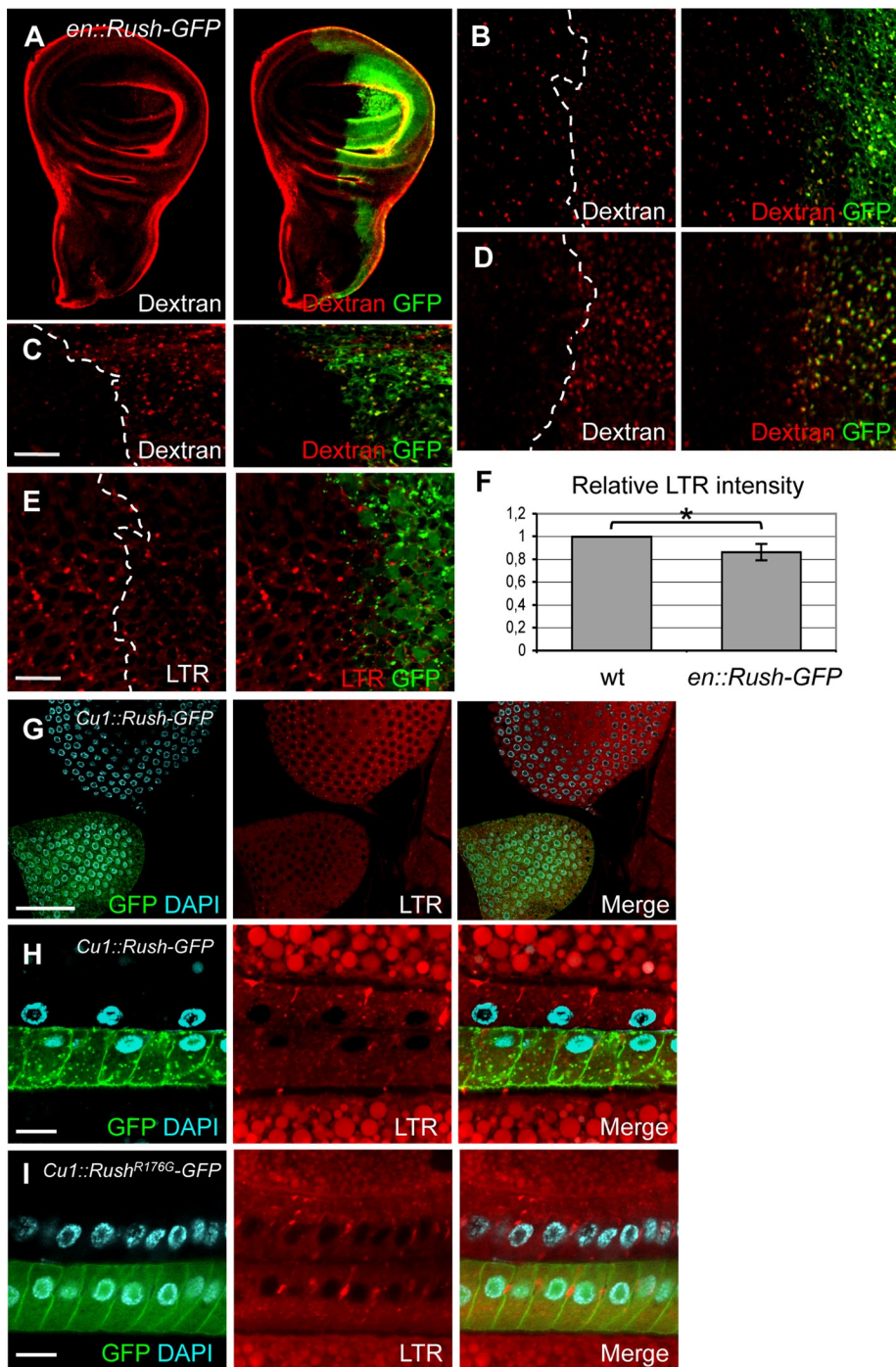
FIGURE 3: Overexpression of Rush-GFP slows the degradation of endocytosed dextran. (A–D) For dextran uptake assays, Rush-GFP was overexpressed in the posterior compartment of wing imaginal disks under control of *en*::GAL4. (B) Five-minute chase, (C) 30-min chase, (D) 60-min chase. (E) LysoTracker staining is decreased in Rush-GFP–overexpressing cells. Quantification is shown in (F). (G and H) LysoTracker (LTR) staining is decreased in follicular cells that overexpress Rush-GFP. Wild-type ovaries and ovaries with Rush-GFP expressed in follicular cells under control of *Cu1*::GAL4 were incubated with LTR. (H) Higher magnification of follicular epithelium of stage 10 egg chambers after incubation with LTR. (I) Expression of Rush[R176G]-GFP, which is unable to localize to endosomes, does not affect LTR staining. (B–E and H–I) Scale bars: 10 μm. (G) Scale bar: 50 μm.

rush genetically interacts with regulators of endocytosis

Since Rush is a highly conserved protein, it is likely that the lack of an obvious loss-of-function phenotype is caused by the redundant activity of other proteins. To test whether *rush[4]* mutant animals are more sensitive to perturbations in other endocytic pathway genes than wild-type flies, we analyzed genetic interactions between *rush* and other regulators of endocytosis. Loss of *rush* decreased survival of animals heterozygous for *Rab5[2]*, a loss-of-function allele of *Rab5* (Figure 5A). While flies heterozygous for *Rab5[2]* and homozygous *rush[4]* mutant flies had wild-type survival levels, deletion of *rush* in the *Rab5[2]* heterozygous background led to decreased viability of flies at embryonic and pupal stages (Figure 5A). Decreased survival rates were partially rescued by ubiquitous expression of Rush-GFP under control of the *armadillo* (*arm*) promoter. A similar effect of *rush* loss was observed in the *hrs[D28]* mutant background. Flies homozygous for *hrs[D28]* die at the early pupal stage (Lloyd *et al.*, 2002). Double mutants of *rush* and *hrs[D28]* never reached the pupal stage, while introduction of *arm*::Rush-GFP rescued the *rush*-induced early lethality.

An opposite effect was observed in genetic interactions with genes that regulate late stages of endocytosis—*carnation* (*car*) and *VhaSFD*. Car is a part of the class C Vps/HOPS complex and regulates the late endosome-to-lysosome transition (Akbar *et al.*, 2009), while VhaSFD is a subunit of vesicular ATPase, which regulates acidification of lysosomes and endocytic trafficking (Yan *et al.*, 2009). Overexpression of *arm*::Rush-GFP reduced eclosion of *car[1]* and *VhaSFD[EY04644]* flies, which was rescued by deletion of *rush* (Figure 5, C and D). Thus loss of *rush* enhances the phenotype of loss-of-function mutations of regulators of early steps of endocytosis (*Rab5* and *hrs*), while Rush overexpression enhances the phenotype of loss-of-function mutations of regulators of late steps of endocytosis (*car* and *VhaSFD*).

Rush modifies the morphology of endosomes

We observed that overexpression of Rush-GFP caused the formation of large vesicle clusters (Figure 6A). To analyze this effect of Rush on endosome morphology, we decided to analyze the effect of Rush overexpression in flies that express Rab5Q88L, which is unable to hydrolyze GTP and is therefore constitutively in its active state (Rab5CA). Rab5 in the active state promotes fusion of endocytic vesicles with early endosomes and the homotypic fusion of separate early endosomes (Gorvel *et al.*, 1991; Rubino *et al.*, 2000). Expression of yellow fluorescent protein (YFP)-Rab5CA in the follicular epithelium induced formation of enlarged early endosomes (Figure 6B), as described previously (Bucci *et al.*, 1992). Endogenous Rush and Rab7 colocalized with Rab5CA endosomes (Figures 6B and S6). Association of late endosome and
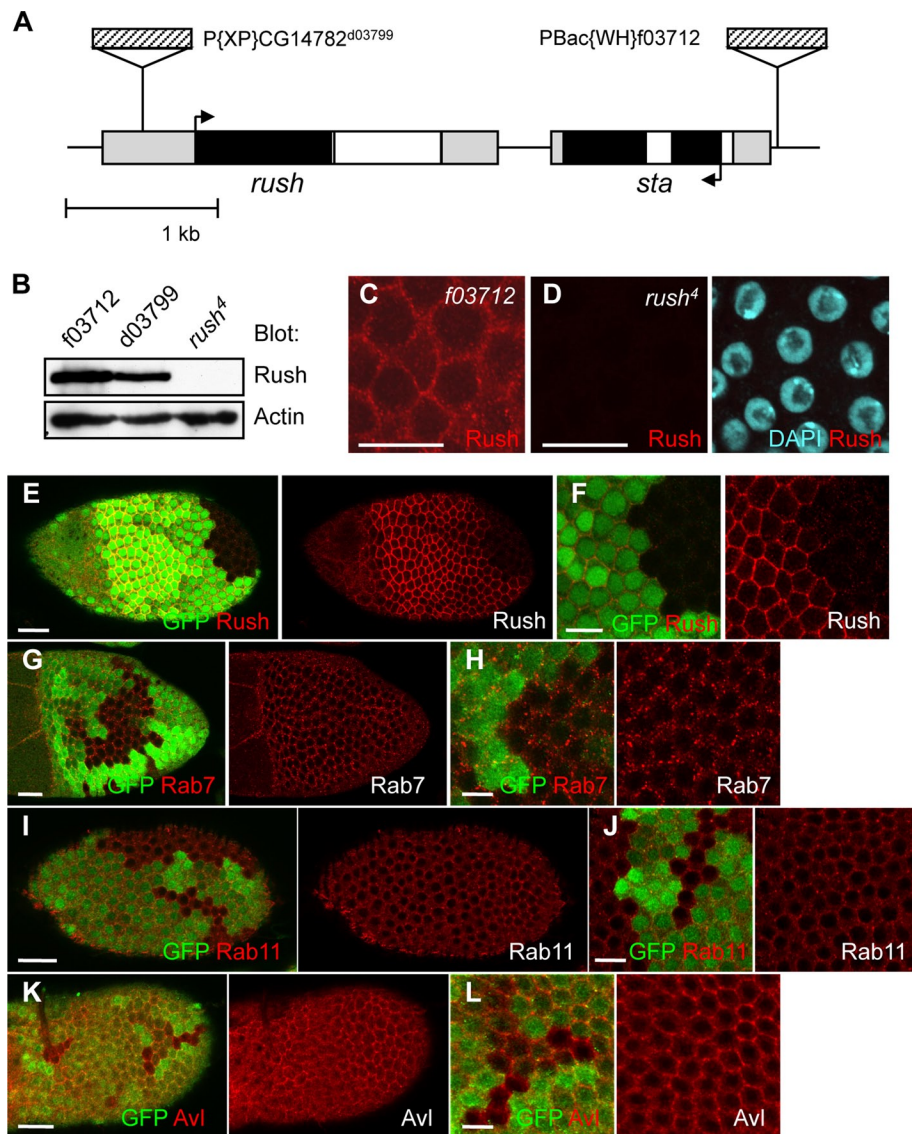
FIGURE 4: Localization of endosomal markers is not affected in clones of *rush* mutant cells. (A) Generation of a *rush* null mutation. *rush* and the downstream gene *sta* were deleted by FLPase-mediated recombination of FRT sites, located in transposons P{XP}CG14782[d03799] and PBac{WH}f03712. The loss of *sta* was rescued by a transgenic construct that contains the genomic sequence of *sta* (Melnick *et al.*, 1993). Transposons are not depicted to scale. 5′ and 3′ UTRs are shown in gray; open reading frames are marked black; introns are white. The translation start site is marked with an arrow. (B) Western blot of fly protein extracts shows loss of the band corresponding to the Rush protein in extracts from homozygous *rush⁴* flies. The transposon insertion lines used to generate the null allele of *rush* were used as positive controls for Rush expression. (C and D) Deletion of *rush* in *rush⁴* mutant flies was confirmed by the loss of anti-Rush immunoreactivity (D) in comparison with the transposon insertion line PBac{WH} f03712 that expresses wild-type levels of Rush (C). (E–L) *rush* follicular cell clones do not show defects in endosomal compartments. (E and F) *rush⁴* follicular cell clones show loss of anti-Rush immunostaining. No differences in the immunostaining against Rab7 (G and H), Rab11 (I and J), and Avl (K and L) were observed in *rush⁴* clones. (E, G, I, and K) Scale bars: 20 μm. (C, D, F, H, J, and L) Scale bars: 10 μm.

of the clustered vesicles (Figure S6, C and D), we conclude that these are clusters of interconnected endosomes and do not represent enlarged intraluminal vesicles of multivesicular bodies. The effect of Rush on endosome morphology depended on the presence of a functional FYVE domain, since Rush[K48E]-GFP caused similar effects to those of the wild-type protein (Figure 6D), while overexpression of Rush[R176G]-GFP had no effect on vesicle shape (Figure 6E). A possible explanation for this phenotype is that overexpressed Rush binds to all accessible PI(3)P molecules in the endosomal membrane and thus inhibits association of Rab5 effectors with endosomes. Two lines of evidence speak against this explanation: First, another FYVE domain protein, Hrs, is still associated with endosomes upon Rush overexpression (Figures S2C and S6, C and D). Second, overexpression of the FYVE domain of Hrs alone did not induce clustering of Rab5CA vesicles (Figure 6F). Mutations that inhibit early endosome fusion lead to a similar clustering phenotype (Rink *et al.*, 2005; Visser Smit *et al.*, 2009), suggesting that overexpression of Rush might inhibit the homotypic fusion of early endosomes.

car loss of function causes clustering of Rush and other endosome markers

Rush overexpression caused formation of enlarged endosomes that contain late endosome markers (Figure 2, D and E), possibly because of defects in fusion with lysosomes as detected by decreased LysoTracker staining (Figure 3, E and F). The class C Vps/ HOPS complex, together with Rab7, regulates the transition between late endosomes and lysosomes. The *car¹* mutation in *carnation*, the fly homologue of Vps33, blocks fusion of late endosomes with lysosomes (Sriram *et al.*, 2003). We first investigated the localization of Rush in the follicular epithelium of *car¹* homozygous mutant animals but did not detect any difference compared with wild type. By contrast, in *car¹* homozygous mutant female germ line cells, Rush was mislocalized to large structures in nurse cells (compare Figure 7D with Figure 7A). We wondered whether this drastic mislocalization was specific for Rush and tested the localization of other endosome markers. Rab7 and, surprisingly, Avl were also found in these large structures (Figure 7, E and F). Endosome-derived yolk vesicles form large round-shaped structures in wild-type oocytes at stage 10 (Figure 7, G and H), whereas they formed irregular clusters of smaller vesicles in *car¹* homozygous mutant oocytes (Figure 7, I and J). Therefore the large structures observed in nurse cells most probably represent compact vesicle clusters. Previous reports have also described clustering of late endosomes caused by a loss of *car*, but in this case early endosome

even lysosome proteins with enlarged Rab5CA vesicles is caused by the inability of early endosomes to transit to the late endosome stage (Rosenfeld *et al.*, 2001; Rink *et al.*, 2005; Wegner *et al.*, 2010). Coexpression of Rush-GFP with YFP-Rab5CA resulted in striking changes of endosome morphology. Rab5-induced large endosomes changed their shape and formed clusters of smaller interconnected vesicles (Figure 6C). Since Hrs was found on the limiting membranes
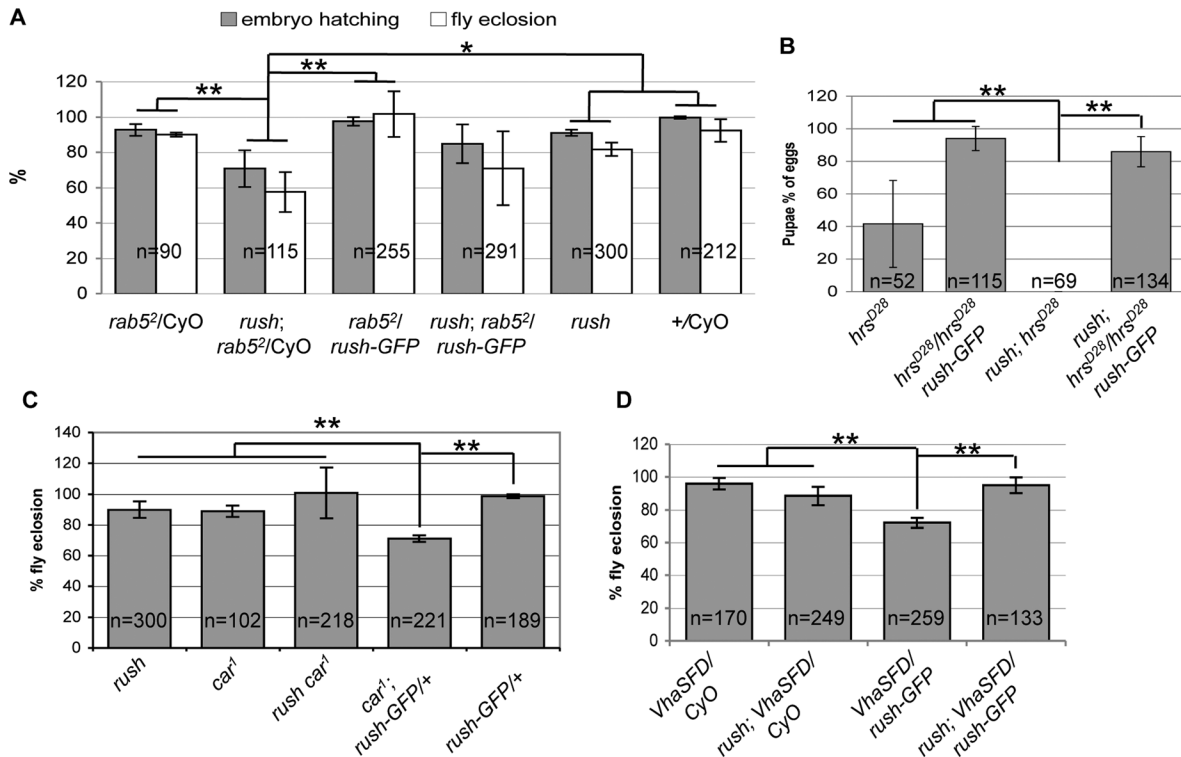
FIGURE 5: *rush* interacts genetically with genes that regulate endocytosis. (A) Loss of *rush* in the *rab5²*/CyO background decreases survival of embryos and pupae. (B) Genetic interaction between *rush* and *hrs^D28*. Overexpression of *arm*::Rush decreases eclosion of *car¹* (C) and *VhaSFD^EY04644* (D) flies. * p < 0.05; ** p < 0.01.

markers like Rab5 only partially colocalized with late endosome clusters (Akbar *et al.*, 2009). Consistent with our observations, downregulation of another member of the HOPS complex, Vps39, caused formation of Rab5 and Rab7 double-labeled endosomes (Rink *et al.*, 2005).

FIGURE 6: Rush overexpression induces clustering of endosomes. (A) A cluster of Rush-GFP–positive vesicles in the follicular epithelium. (B) Rush localizes to Rab5CA-induced enlarged endosomes. (C) Overexpression of Rush together with Rab5CA causes clustering of endosomes. (D) The Rush^K48E mutant is able to induce endosome clustering, while the Rush^R176G mutant, which is unable to localize to endosomes, does not affect Rab5CA endosome shape (E). (F) Overexpression of the Hrs FYVE domain does not lead to Rab5CA endosome clustering. Scale bars = 10 μm.

The *car¹* endosome-clustering phenotype was similar to the phenotype observed upon Rush overexpression, which also caused clustering of Rab7-positive vesicles (Figures 2, D and E, and 6A). Therefore it appears possible that Rush counteracts Car function. Support for this hypothesis comes from genetic interaction studies, which showed that overexpression of Rush enhances the *car¹* mutant phenotype (Figure 5C).
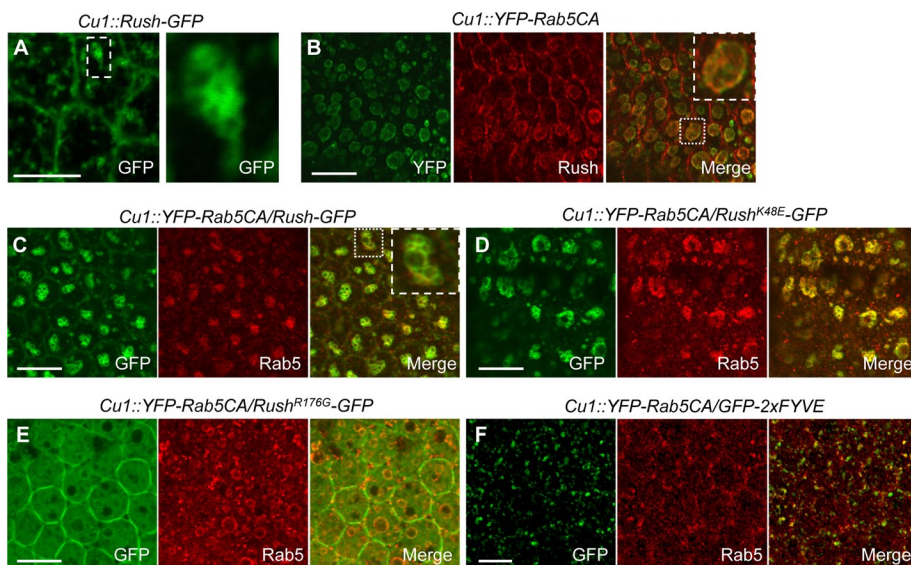
Dor is required for Rush protein stability

We next sought to verify whether Vps18, another member of the class C Vps/HOPS complex, affects Rush localization. *dor⁸* is a strong allele of *deep orange* (*dor*), the fly Vps18 homologue, which leads to decreased Dor protein amounts and disrupts Dor function (Akbar *et al.*, 2009). Clones of *dor⁸* cause clustering of Hrs- and Rab7-positive endosomes, in a manner similar to the *car¹* phenotype (Figure 8A). Unexpectedly, the immunfluorescence signal for Rush was strongly reduced in *dor⁸* follicular and germ line cell clones (Figure 8, B and C). This could be caused either by mislocalization of Rush to the cytoplasm or by reduction of Rush protein levels. To test the latter possibility, we analyzed protein extracts from *dor⁸* germ line clones and found that the protein amount was strongly reduced in comparison with control clones (Figure 8, E and F). Thus Dor is required to maintain normal levels of Rush protein.
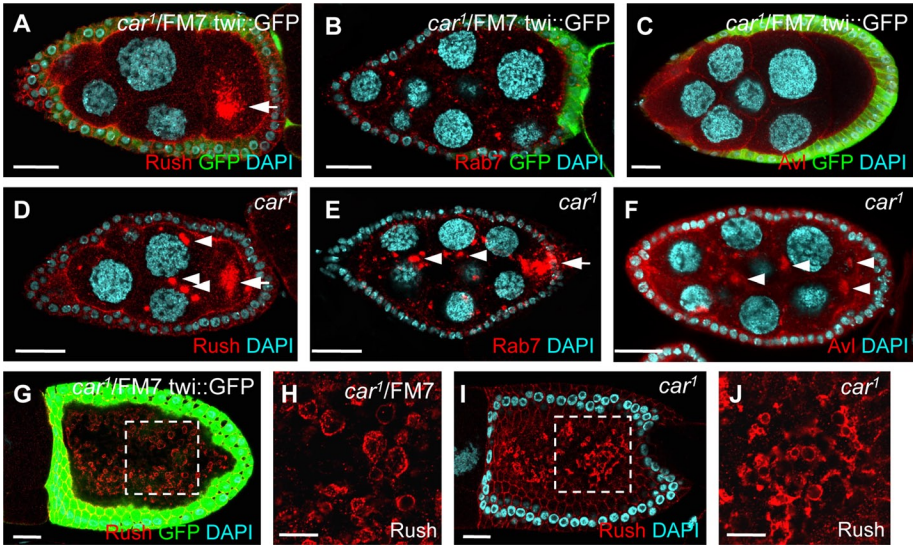
FIGURE 7: *car* is required for proper localization of endosomes and interacts genetically with *rush*. (A–C) Wild-type localization of Rush (A), Rab7 (B), and Avl (C) in *car¹*/FM7 *twi*-GFP heterozygous ovaries. (D–F) *car¹* homozygous flies show accumulations of Rush (D), Rab7 (E), and Avl (F) in nurse cells. Endosome clusters in *car¹* mutant ovaries are marked with arrowheads. Accumulations of endosomes in the oocyte, which are typical for stage 7–8 wild-type oocytes (Tanaka and Nakamura, 2008), are marked with arrows. (G) Rush localizes to yolk granules in the *car¹*/FM7 *twi*-GFP oocyte at stage 10. (H) Magnification of the marked area in (G). (I) Oocytes hemizygous mutant for *car¹* form yolk granule clusters. (J) Magnification of the marked area in (I). (A–G and I) Scale bars: 20 μm. (H and J) Scale bars: 10 μm.

Rush recruits Rab GDI to the endosomal membrane

Rush has multiple effects in the endocytic pathway, including regulation of late endosome formation and regulation of endosome morphology. Endosome formation is regulated by Rabs that are associated with the endosome membrane in the active GTP-bound form and become released into the cytosol after hydrolysis of GTP to GDP. In this inactive state, Rabs associate with GDI, which delivers the inactive Rab back to the target membrane, where it can be activated again. We wondered whether the effects of Rush on endosomal trafficking could be caused by changes in the Rab activation cycle. Pulldown experiments with purified GST- or maltose-binding protein (MBP)-tagged Rush and GDI showed that the proteins can directly interact with one another (Figure 9, A–D). In S2 cells, endogenous Rush localized to the cortex and in intracellular punctae (Figure 9, E and F). When expressed in S2 cells, GFP-GDI was localized in the cytosol, as expected (Figure 9F). On overexpression of Rush, the protein accumulated asymmetrically at the plasma membrane (Figure 9, G–I). GFP-GDI became
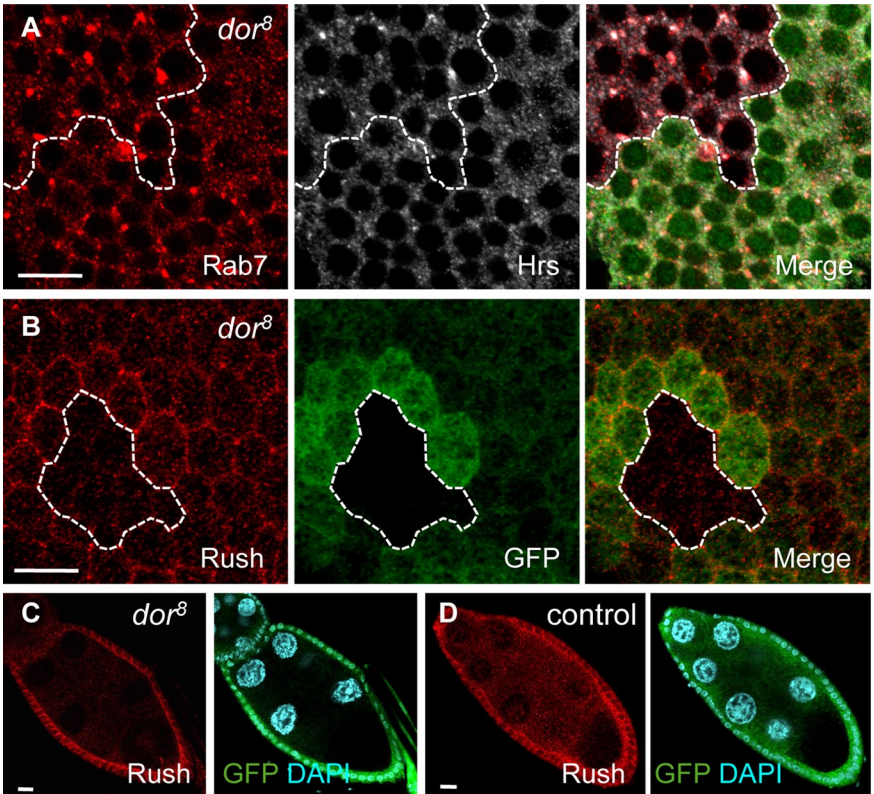

FIGURE 8: Dor regulates Rush protein levels. (A) in *dor⁸* follicular cell clones Hrs and Rab7 form endosome clusters. Staining for Rush is decreased in *dor⁸* mutant clones in follicular epithelium (B) and germ line (C). (D) Rush staining is visible in control germ line clone. Lack of GFP marks mutant clones. (E) Rush protein levels are decreased in protein extracts from *dor⁸* germ line clone ovaries. Extracts from *rush* and control germ line clones are shown for comparison. (F) Quantification of (E). Error bars represent SD of three independent experiments. GLC, germ line clones. (A–D) Scale bars: 10 μm.
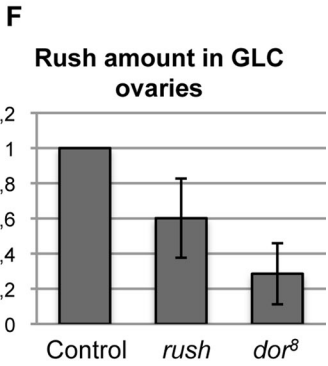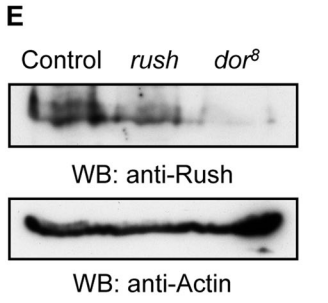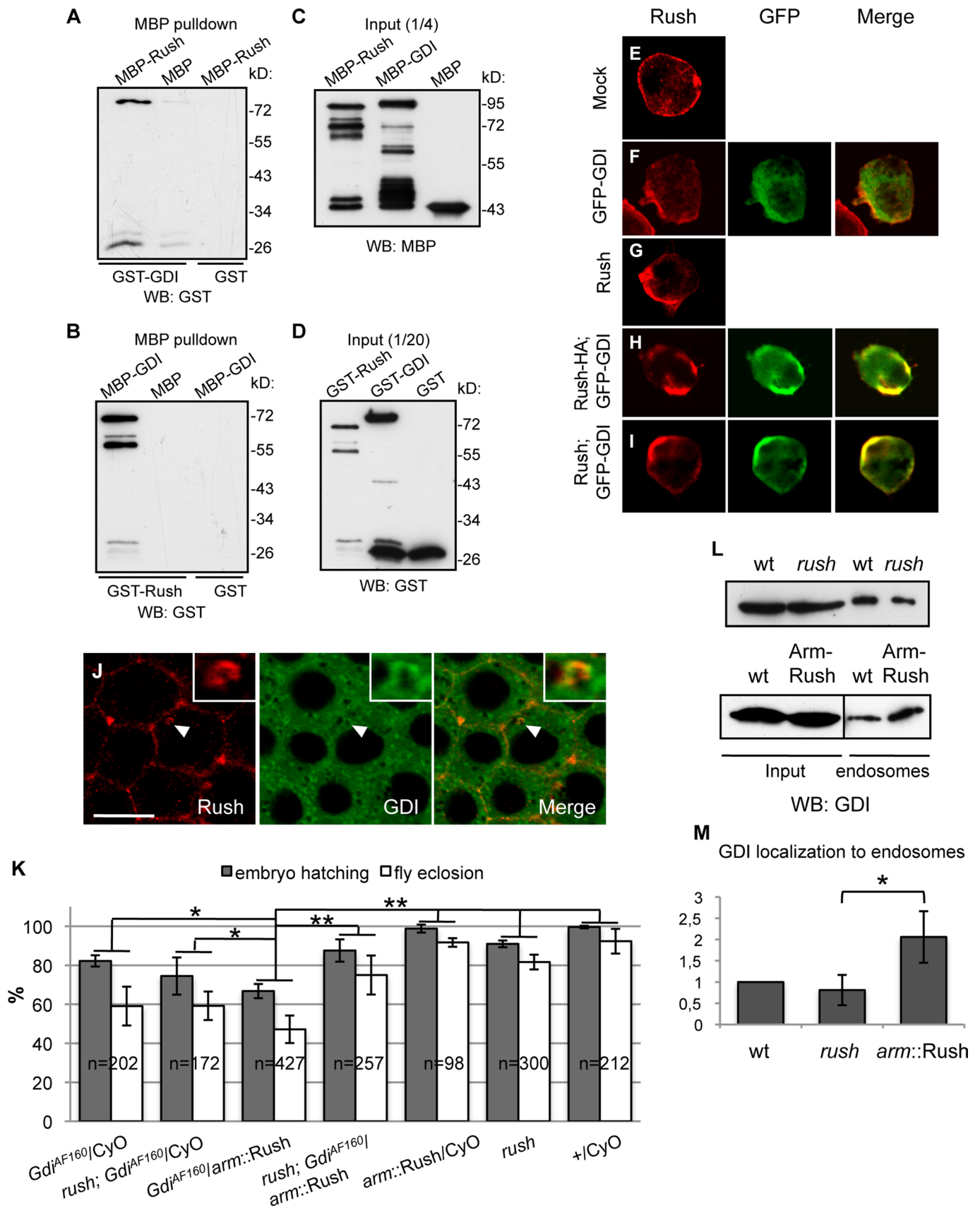
FIGURE 9: Rush interacts with GDI and recruits GDI to endosomal membranes. (A–D) Purified recombinant Rush and GDI proteins interact directly. MBP-fusion proteins were bound to amylose beads and incubated with GST-tagged proteins or with GST alone. Proteins that were precipitated together with the beads were analyzed by Western blotting. (A) GST-GDI precipitates with MBP-Rush, but not with MBP. GST was used as negative control. (B) GST-Rush precipitates

relocalized to the accumulations of overexpressed Rush, pointing to a direct interaction of Rush and GDI in S2 cells (Figure 9, H and I). When GFP-GDI was expressed in the follicular epithelium, it localized to the cytosol and to the plasma membrane and partially colocalized with endogenous Rush on intracellular vesicles (Figure 9J, inset).

To test whether *rush* and *Gdi* interact genetically, we analyzed the effect of *rush* mutation or overexpression in heterozygous *Gdi[AF160]* loss-of-function mutants (Figure 9K; Ricard *et al.*, 2001). While loss of *rush* did not affect survival of heterozygous *Gdi[AF160]* flies, Rush-GFP overexpression led to decreased viability of *Gdi[AF160]* heterozygous mutants. The viability of *Gdi[AF160]* heterozygous flies that overexpress Rush-GFP was rescued by removal of both copies of endogenous *rush* (Figure 9K). A fraction of mammalian GDI is associated with endosomal membranes (Ullrich *et al.*, 1993). When we performed sucrose gradient fractionation of S2 cells, both Rush and GDI were found associated with endosomes (Figure 1I). Since Rush was able to recruit GDI to the membrane in S2 cells, we hypothesized that increased levels of Rush might cause entrapment of GDI at the endosomal membrane and thus hamper GDI function. Indeed, we found that the amount of GDI on endosomal membranes increased upon Rush-GFP overexpression, while *rush* mutant animals showed slightly decreased levels of endosomal GDI (Figure 9L). To quantify these results, the amount of GDI in the endosomal fraction was normalized over the input and compared with the wild type (Figure 9M).

DISCUSSION

Rush is an endosomal protein
We have identified Rush as a previously uncharacterized endosomal protein, which upon overexpression affects endosomal trafficking downstream of early endosomes. Since *rush* mutants are homozygous viable and endosomal markers are normal in *rush* mutant cells, Rush may function redundantly with other factors in this process. Phafin2, the human homologue of Rush, has been shown to increase the binding of Rab5 to its effectors as monitored by a fluorescence resonance energy transfer (FRET) assay with the Rab5-binding domain of Rabaptin5 (Lin *et al.*, 2010). Dominant-negative Rab5 disrupted formation of Phafin2-induced large endosomes, positioning Rab5 activity upstream of Phafin2 (Lin *et al.*, 2010). Epithelial cells that overexpress Rush contain enlarged vesicles that show markers of both early and late endosomes. Since Rab7 is recruited to endosomes by Rab5-GTP, large Rab7-positive endosomes in Rush-overexpressing cells might be an effect of excessive Rab5 activation (Figure S7). *rush* homozygous mutant flies that were

at the same time heterozygous for *Rab5[2]* showed reduced viability compared with *rush* homozygous mutant or *Rab5[2]* heterozygous mutant flies, pointing to a functional interaction between Rush and Rab5. Alternatively, this result might also be explained by a cumulative effect of two mutations affecting different steps of the endocytic pathway.

The function of Rush in regulation of endocytic trafficking
Overexpression of Rush caused the formation of enlarged Rab7-positive endosomes and reduced the degradation of endocytosed dextran, which became accumulated in endosomes. Decreased LysoTracker staining suggests that Rush overexpression might downregulate late endosome to lysosome traffic. Mutants for *Drosophila* V-ATPase, a proton pump necessary for acidification of the lysosomal lumen, also develop enlarged late endosomes and show decreased LysoTracker staining (Yan *et al.*, 2009). Rush overexpression decreased the survival of animals carrying mutations in genes necessary for late endosome fusion with lysosomes (*car*) and lysosome acidification (*VhaSFD*), suggesting that both processes might be regulated by Rush.

An additional reason for the increased endosome size induced by Rush overexpression could be a defect in the transition from early to late endosomes, especially since the enlarged endosomes appear to harbor both early and late endosome markers (Rink *et al.*, 2005). Increased recruitment of GDI to early endosomes could lead to excessive activation of Rab5 and increased endosome size, as well as recruitment of Rab7 to these endosomes. Increased late endosome size could also be caused by defects in endocytic recycling, thus directing all endocytosed material for degradation. However, the size of Rab11-marked recycling endosomes was not affected in *rush* mutant cells or upon Rush overexpression. Thus the Rush-mediated effects on late endosome morphology are most probably not caused by defects in recycling of endocytosed proteins.

The function of Rush in endosome shape regulation
Overexpression of Rush led to formation of endosome clusters that were similar to the those seen with the *car[1]* mutation. This phenotype might be caused by a defect in vesicle fusion, although vesicle docking still takes place successfully. The early endosomal protein Hrs has been found to promote the transition to late endosomes by inhibiting the homotypic fusion of early endosomes (Sun *et al.*, 2003; Visser Smit *et al.*, 2009). Inhibition of the early endosome fusion leads to clustering of early endosomes that resembles the effect of Rush on Rab5CA-induced early endosomes (Visser Smit *et al.*, 2009). The similarity of phenotypes suggests a possible

with MBP-GDI, but not with MBP. GST was used as negative control. (C) Input for MBP-fusion proteins. (D) Input for GST-fusion proteins. (E–I) Rush overexpression changes the intracellular localization of GDI in S2 cells. S2 cells were transfected with GFP-GDI alone or together with hemagglutinin-tagged Rush (Rush-HA), and the localization of proteins was observed. (E–F) Endogenous Rush localizes to the cortex, while GFP-GDI is mainly localized in the cytosol (F). (G) Overexpressed Rush shows increased localization at the cortex. (H–I) Overexpressed Rush (I) and Rush-HA (H) recruit GFP-GDI to the cortex. (J) Localization of GFP-GDI and endogenous Rush in the follicular epithelium of a stage 10 egg chamber. The Rush-positive vesicle marked by the arrowhead is magnified in the inset. Scale bar: 10 μm. (K) Overexpression of arm::Rush-GFP in *gdi[AF160]* heterozygous flies reduces the hatching rate of embryos and pupae. (L) GDI levels at endosomal membranes are affected by Rush expression. Lysates of wild-type, *rush* mutant, and arm::Rush-GFP–overexpressing embryos were subjected to discontinuous sucrose gradient ultracentrifugation to separate early endosomes. The GDI fraction that was bound to endosomes was analyzed by Western blot. (M) The amount of GDI on endosomal membranes was quantified as follows: the signal intensity of input and endosomal fractions was measured with Adobe Photoshop. The intensity of the endosomal GDI fraction was divided by the input GDI and normalized over the similarly calculated intensity of the Rab5 fraction in endosomes. Wild-type GDI levels were converted to 1, and the changes of GDI in the endosomal fraction in *rush* mutant or arm::Rush-GFP embryos were calculated in comparison with the wild type. Quantification was done with results from three independent experiments. * $p < 0.05$.

interaction between Rush and Car at this step. Most probably Rush blocks vesicle fusion, while the Car homologue Vps33 is required for vesicle docking (Ostrowicz et al., 2010) and fusion pore opening (Pieren et al., 2010). In our experiments, the car¹ mutation led to clustering of early endosomes, as marked by the early endosomal syntaxin Avl. This observation is in contrast to previously published results, in which separate clusters of early and late endosomes were observed in carΔ146 null mutant wing disk cells (Akbar et al., 2009). This discrepancy might arise either from different cell types tested (germ line cells vs. wing disk cells) or from the nature of mutations. car¹, the allele we used here, is a weak loss-of-function allele (Sriram et al., 2003), whereas the previously published experiments in wing disks were done with clones of the null allele carΔ146. We wanted to address this issue by including the null allele carΔ146 in our analyses, but unfortunately we were not able to obtain this stock.

The presence of early endosome markers in the abnormal endosomes observed in car¹ mutant germ line cells is not completely unexpected, because the Car homologue Vps33 is also a member of the CORVET complex, which is involved in the regulation of early endosome fusion (Richardson et al., 2004; Peplowska et al., 2007). A knockdown of another HOPS complex member, Vps39, also causes colocalization of markers of early and late endosomes (Rink et al., 2005).

Role of Dor in Rush stabilization
We found that Dor is necessary to maintain normal Rush protein levels, suggesting that Rush and Dor might form a protein complex. Interestingly, the car¹ mutation did not reduce Rush protein levels, but caused accumulation of Rush in endosome clusters, together with other endosome markers. Two explanations for the different effect of the two class C Vps/HOPS complex members are possible. First, Car has been described as being necessary for removal of Dor on maturing late endosomes (Sriram et al., 2003). It can be imagined that Car might act similarly in removal of Rush from endosomes, which also explains why overexpression of Rush in animals with compromised Car function decreases fly viability. Interestingly, overexpression of Dor also enhances the car¹ phenotype (Sriram et al., 2003). Second, it is possible that the mutant Car protein encoded by car¹ is still able to stabilize Rush and that a null allele of car would also result in destabilization of Rush.

Interaction between Rush and GDI
Rush is able to directly bind GDI, recruits GDI to the cell membrane in S2 cells, and localizes together with GDI on endosomal membranes. Overexpression of Rush increases the amount of GDI that is bound to the endosomal membrane. Therefore Rush could affect the activation cycle of Rabs by regulating the localization of GDI. Overexpression of Rush decreases the survival of Gdi^AF160 heterozygous mutant animals, possibly by titrating out the decreased cytosolic pool of GDI. Recycling of Rabs might be limited if an increased amount of GDI associates with endosomes.

Since GDI can interact with all Rab proteins involved in endosomal trafficking, the mechanistic consequences of its binding to Rush are difficult to interpret. Rush-GDI interaction might cause overactivation of Rab5 or Rab7. The available data on Rush function could be explained by one of the following scenarios: Rab5 gets overactivated by GDI that is trapped on endosomes (Figure S7). Subsequently, active Rab5 mediates recruitment of the class C Vps/HOPS complex and Rab7 to endosomes and thus drives the transition from early to late endosomes (Nordmann et al., 2010; Poteryaev et al., 2010). Prolonged activity of Rab5 leads to organelles containing both early and late endosome components (Avl, Hrs, Rab7; Rosenfeld

et al., 2001; Rink et al., 2005; Wegner et al., 2010). Alternatively, large late endosomes may be formed by overactivation of Rab7, but this model does not explain the localization of early endosome components to late endosomes as a consequence of Rush overexpression, as well as the decreased LysoTracker staining, since Rab7 promotes fusion of late endosomes with lysosomes (Bucci et al., 2000).

To clarify these issues, it will be important to monitor the activity states of the different Rab proteins involved in the endosomal trafficking steps affected by Rush loss of function and overexpression, for instance by live imaging using specific FRET probes. Since Rush is highly conserved in evolution and its human homologue Phafin2 does affect endosomal trafficking as well, we expect to gain significant knowledge from future studies on its function in flies and mammals.

MATERIALS AND METHODS
Fly stocks and genetics
The following stocks were used in this study: P{XP}CG14782^d03799 and PBac{WH}f03712 were from the Exelixis collection (Harvard University, Cambridge, MA); w^1118: UASp-YFP-Rab5Q88L (#9774), UASp-YFP-Rab5 (#24616), UASp-YFP-Rab7 (#23641), UASp-YFP-Rab11/TM3 (#9790); w^1: noc^Sco/SM6b hsFLP (#6876); dpp^s1 Gdi^AF160 b^1 cn^1 bw^1/SM1 (#6473), Hrs^D28 cn^1 bw^1 sp^1/In(2LR)Gla, wg^Gla-1 (#3914), y^1 w^67c23; P{EPgy2}VhaSFD^EY04644/CyO (#15758), car^1 (#19), dor^8/FM6 (#28); w*: w* f^1 P{FRT(w^hs)}9-2 (#5749), y^1 w^1118 P{Ubi-GFP. nls}P{FRT(w^hs)}9-2 (#5832), P{FRT(w^hs)}9-2; P{hsFLP}38 (#1843); and P{GAL4-arm.S}11 (#1560) were from Bloomington Drosophila stock center (stock numbers given in parentheses; Bloomington, IN). y w and Rab5²/CyO, GFP-2xFYVE (Wucherpfennig et al., 2003); C(1)DX y f/sta^lt3/Y; Tr1 (Melnick et al., 1993), and Cu1::GAL4 (Queenan et al., 1997) were sourced as noted in references. The rush^4 null allele was generated by FLP/FRT-mediated recombination in trans of the P{XP}CG14782^d03799 and PBac{WH}f03712 transposon insertions as described in Parks et al. (2004). Transgenic flies were generated as described in Bachmann and Knust (2008). Follicular cell clones and germ line clones for rush and dor^8 were generated as described using a heat-shock promoter–driven flippase on the second chromosome (Chou and Perrimon, 1996).

Molecular biology
The coding region of rush was amplified using primers 5'-CACC-ATGGTGGACCGTCTGGTCAACTCG-3' and 5'-ACAGTGGCT-GCCCGTCGTCG-3'. GDI was amplified from wild-type fly cDNA with primers 5'-CACCAATGAGGAATACGATGCGATTG-3' and 5'-TTACTGCTCCTCGTCACCCAACTCG-3'. PCR products were cloned into pENTR vector using the pENTR Directional TOPO Cloning Kit (Invitrogen, Carlsbad, CA). For expression in S2 cells and for generation of transgenic flies, constructs were recombined into different expression vectors (pAWH, pAW, and pTWG for rush; pAGW and pTGW for GDI; Murphy lab, Carnegie Institution of Washington, Baltimore, MD) using Gateway technology (Invitrogen). For expression as a GST-fusion protein, rush was cloned into pGEX-4T-1 (GE Healthcare, Piscataway, NJ) using BamHI and EcoRI, and GDI was cloned into pGGWA (Busso et al., 2005). For generation of MBP-fusion proteins, rush and GDI were cloned into pMGWA (Busso et al., 2005). The PH domain of Rush was amplified using primers: 5'-GAGGATCCCT-GGTGGGCGAGGGC-3' and 5'-GAGAATTCTCACAGGTCCTC-CACGCAC-3'. Primers used for amplification of the FYVE domain of Rush were: 5'-CTGGATCCAACCACGCCGCCGTTTGGG-3' and 5'-GTGAATTCTCAGTGCTTCAAGCGCTCGTAGC-3'. PCR products were cloned into pGEX-4T-1 vector (GE Healthcare) using BamHI and EcoRI.

Point mutations were introduced into the *rush* sequence with QuikChange II Site-Directed Mutagenesis kit (Stratagene, Agilent, Santa Clara, CA) according to the manufacturer's instructions. Primers used to introduce the K48E mutation in the *rush* PH domain were 5'-CCAAGATGTGTCGCGAGCGGCCCAAGTCG-3' and 5'-CGACT-TGGGCCGCTCGCGACACATCTTGG-3'. The R176G mutation in the FYVE domain of *rush* was introduced with primers: 5'-GCATCACT-GCGGCAACTGCGGCGCTGTTG-3' and 5'-CAACAGCGCCGCAG-TTGCCGCAGTGATGC-3'.

Antibodies, immunohistochemistry, dextran uptake assay, LysoTracker assay, and image analysis

Antibodies against Rush were generated by immunizing two rabbits with the peptides VDRLVNSEANTRRIAC (aa 2–16) and PGGESH-DEPRFYGDN (aa 256–270). Final bleeds were pooled and affinity-purified against the peptide corresponding to amino acids 2–16 (Eurogentec, Saraig, Belgium). For immunohistochemical stainings, the following primary antibodies were used: rabbit anti-Rush, affinity-purified, 1:1000 (this study); mouse anti-GFP, 1:1000 (A11120; Invitrogen, Carlsbad, CA); rabbit anti-Rab7, 1:3000 (Tanaka and Nakamura, 2008); chicken anti-Avl, 1:500 (Lu and Bilder, 2005); rabbit anti-Rab5, 1:1000 (Tanaka and Nakamura, 2008); rabbit anti-Rab11, 1:3000 (Tanaka and Nakamura, 2008); guinea pig anti-Hrs, 1:500 (Lloyd et al., 2002). Secondary antibodies conjugated to Cy2, Cy3 (Jackson ImmunoResearch Europe, Newmarket, UK), and Alexa Fluor 647 (Invitrogen) were used at 1:400 dilution. DNA was stained with 4',6-diamidino-2-phenylindole (DAPI; Invitrogen). Ovaries were fixed with 4% formaldehyde in phosphate-buffered saline (PBS; pH 7.4). For staining with anti-Rush antibody, a fixation solution of the following composition was used: 4% formaldehyde, 75 mM PIPES, 15% picric acid. For LysoTracker staining, ovaries and wing disks were dissected in PBS and incubated with 50 µM LysoTracker DND-99 (Invitrogen) in PBS for 3 min in the dark. The samples were then washed three times with PBS and fixed as described in the preceding paragraph. After being washed repeatedly in PBS, samples were mounted on microscope slides. Dextran uptake assays in wing imaginal disks were performed essentially as described in Entchev et al. (2000) with the following modifications: all steps were performed in Schneider 2 medium and Alexa Fluor 568 dextran (MW10000, fixable; Invitrogen) was used. Images were taken with a Zeiss LSM 510 Meta confocal microscope (Jena, Germany) and processed using Adobe Photoshop (San Jose, CA). For measurements of endosome size, images were analyzed with ImageJ software (National Institutes of Health, Bethesda, MD). Images were converted to 8-bit grayscale, inverted, and processed with manual thresholding. Mean particle sizes of each image were measured with the Analyze Particles function of ImageJ. Maximal particle diameter was set to 900 pixels to avoid detection of nearby endosomes or the plasma membrane as one particle. Statistical significance was calculated with a two-tailed Student's *t* test. For colocalization analysis, images were converted to 8-bit grayscale and processed with the Colocalization Threshold plug-in of ImageJ. The plug-in yielded a Pearson's correlation coefficient (Rtotal). Pearson's coefficient represents intensity correlation of all non-zero-zero pixels that overlay in images of two channels. Values of Pearson's coefficient ranged from −1 (no correlation between pixel intensities in two channels) to +1 (linear relationship between pixel intensity values of two channels).

Lipid overlay assay

To determine lipid-binding specificity of Rush and its separate domains, PIP Strips (Echelon Biosciences, Salt Lake City, UT) were used

according to the manufacturer's protocol. In brief, the membrane was blocked (Tris-buffered saline [TBS], 0.1% Tween, 3% bovine serum albumin) for 1 h at room temperature and incubated for 1 h with 0.2 µg/ml GST-fusion protein in blocking buffer. The membrane was washed three times in TBS with 0.1% Tween, and the bound GST-fusion protein was detected by incubation with rabbit anti-GST antibody (G7781; Sigma-Aldrich, Steinheim, Germany), which was followed by a horseradish peroxidase–conjugated goat anti–rabbit secondary antibody (Jackson ImmunoResearch Europe, Newmarket, UK) and chemiluminescence reaction (Roche, Mannheim, Germany).

Purification of endosomes

Early and late endosomes were separated via density gradient centrifugation as described in Torres et al. (2008), with modifications. In brief, S2 cells were harvested by centrifugation at 1000 rpm at 4°C, washed once in 10 ml of ice-cold PBS, and resuspended 1:4 in homogenization buffer (250 mM sucrose, 3 mM imidazole, pH 7.5). Cells were homogenized by passing them 10 times through a 26-gauge needle in a 1-ml syringe. Postnuclear supernatant (PNS) was separated by centrifugation for 15 min at 3500 rpm at 4°C. PNS was diluted 2:3 with 60% sucrose in homogenization buffer to achieve a final sucrose concentration of 40.6%. A discontinuous sucrose gradient was prepared by sequentially overlaying 1 ml of PNS, 40.6% sucrose with 2 ml of 35% sucrose in 3 mM imidazole (pH 7.5), 1.5 ml of 25% sucrose in 3 mM imidazole (pH 7.5), and 400 µl of homogenization buffer (8% sucrose) in a Beckman 5-ml centrifge tube. The gradient was centrifuged at $125,000 \times g$ at 4°C in an Optima MAX ultracentrifuge (Beckman Coulter, Brea, CA). Fraction 1 was collected at the 35/25% sucrose interface and fraction 2 at the 8/25% sucrose interface. Protein distribution in endosomal fractions was analyzed by Western blotting.

Protein pulldowns

GST- and MBP-fusion proteins were expressed in BL21-competent bacterial cells and purified with glutathione Sepharose beads (GE Healthcare, Piscataway, NJ) or amylose resin (New England Biolabs, Ipswich, MA). Amylose resin with bound MBP-Rush, MBP-GDI, or MBP was incubated with equal amounts of GST-GDI, GST-Rush, or GST alone in pulldown buffer (150 mM NaCl, 10 mM $MgCl_2$, 20 mM HEPES, 1 mM EDTA, 1% Triton X-100, 5 mM dithiothreitol) for 1 h at room temperature.

Western blots

Fly lysates were prepared in TNT buffer (150 mM NaCl; 50 mM Tris, pH 8.0; 1% Triton X-100) supplemented with protease inhibitors (Roche, Mannheim, Germany). Western blots were performed as described in Wodarz (2008). Antibodies used for Western blots were: rabbit anti-actin, 1:1000 (A2066; Sigma-Aldrich, Steinheim, Germany); rabbit anti-GST, 1:20000 (G7781; Sigma-Aldrich); rabbit anti-GDI2 (AV13037; Sigma-Aldrich); mouse anti-MBP, 1:20000 (E8032S; New England Biolabs, Ipswich, MA); rabbit anti-Rush, affinity-purified, 1:1000 (this study); rabbit anti-Lva, 1:1000 (Sisson et al., 2000); rabbit anti-Rab5, 1:1000 and rabbit anti-Rab7, 1:1000 (Tanaka and Nakamura, 2008). The protein amount in bands was quantified with Adobe Photoshop (San Jose, CA).

REFERENCES

Akbar MA, Ray S, Kramer H (2009). The SM protein Car/Vps33A regulates SNARE-mediated trafficking to lysosomes and lysosome-related organelles. Mol Biol Cell 20, 1705–1714.

Bachmann A, Knust E (2008). The use of P-element transposons to generate transgenic flies. Methods Mol Biol 420, 61–77.

Bucci C, Parton RG, Mather IH, Stunnenberg H, Simons K, Hoflack B, Zerial M (1992). The small GTPase rab5 functions as a regulatory factor in the early endocytic pathway. Cell 70, 715–728.

Bucci C, Thompsen P, Nicoziani P, McCarthy J, van Deurs B (2000). Rab7: a key to lysosome biogenesis. Mol Biol Cell 11, 467–468.

Busso D, Delagoutte-Busso B, Moras D (2005). Construction of a set Gateway-based destination vectors for high-throughput cloning and expression screening in Escherichia coli. Anal Biochem 343, 313–321.

Cavalli V, Vilbois F, Corti M, Marcote MJ, Tamura K, Karin M, Arkinstall S, Gruenberg J (2001). The stress-induced MAP kinase p38 regulates endocytic trafficking via the GDI:Rab5 complex. Mol Cell 7, 421–432.

Chen W, Li N, Chen T, Han Y, Li C, Wang Y, He W, Zhang L, Wan T, Cao X (2005). The lysosome-associated apoptosis-inducing protein containing the pleckstrin homology (PH) and FYVE domains (LAPF), representative of a novel family of PH and FYVE domain-containing proteins, induces caspase-independent apoptosis via the lysosomal-mitochondrial pathway. J Biol Chem 280, 40985–40995.

Chen X et al. (2002). Gene expression patterns in human liver cancers. Mol Biol Cell 13, 1929–1939.

Chotard L, Mishra AK, Sylvain MA, Tuck S, Lambright DG, Rocheleau CE (2010). TBC-2 regulates RAB-5/RAB-7-mediated endosomal trafficking in Caenorhabditis elegans. Mol Biol Cell 21, 2285–2296.

Chou TB, Perrimon N (1996). The autosomal FLP-DFS technique for generating germline mosaics in Drosophila melanogaster. Genetics 144, 1673–1679.

Currie RA, Walker KS, Gray A, Deak M, Casamayor A, Downes CP, Cohen P, Alessi DR, Lucocq J (1999). Role of phosphatidylinositol 3,4,5-trisphosphate in regulating the activity and localization of 3-phosphoinositide-dependent protein kinase-1. Biochem J 337, 575–583.

Dowler S, Currie RA, Campbell DG, Deak M, Kular G, Downes CP, Alessi DR (2000). Identification of pleckstrin-homology-domain-containing proteins with novel phosphoinositide-binding specificities. Biochem J 351, 19–31.

Entchev EV, Schwabedissen A, Gonzalez-Gaitan M (2000). Gradient formation of the TGF-β homolog Dpp. Cell 103, 981–991.

Feng Y, Press B, Wandinger-Ness A (1995). Rab 7: an important regulator of late endocytic membrane traffic. J Cell Biol 131, 1435–1452.

Gaullier JM, Ronning E, Gillooly DJ, Stenmark H (2000). Interaction of the EEA1 FYVE finger with phosphatidylinositol 3-phosphate and early endosomes. Role of conserved residues. J Biol Chem 275, 24595–24600.

Gillooly DJ, Simonsen A, Stenmark H (2001). Cellular functions of phosphatidylinositol 3-phosphate and FYVE domain proteins. Biochem J 355, 249–258.

Gorvel JP, Chavrier P, Zerial M, Gruenberg J (1991). rab5 controls early endosome fusion in vitro. Cell 64, 915–925.

Grosshans BL, Ortiz D, Novick P (2006). Rabs and their effectors: achieving specificity in membrane traffic. Proc Natl Acad Sci USA 103, 11821–11827.

Hickey CM, Wickner W (2010). HOPS initiates vacuole docking by tethering membranes before trans-SNARE complex assembly. Mol Biol Cell 21, 2297–2305.

Januschke J, Nicolas E, Compagnon J, Formstecher E, Goud B, Guichet A (2007). Rab6 and the secretory pathway affect oocyte polarity in Drosophila. Development 134, 3419–3425.

Kim Y, Ikeda W, Nakanishi H, Tanaka Y, Takekuni K, Itoh S, Monden M, Takai Y (2002). Association of frabin with specific actin and membrane structures. Genes Cells 7, 413–420.

Kinchen JM, Ravichandran KS (2010). Identification of two evolutionarily conserved genes regulating processing of engulfed apoptotic cells. Nature 464, 778–782.

Kutateladze TG ((2006). Phosphatidylinositol 3-phosphate recognition and membrane docking by the FYVE domain. Biochim Biophys Acta 1761, 868–877.

Li C, Liu Q, Li N, Chen W, Wang L, Wang Y, Yu Y, Cao X (2008). EAPF/Phafin-2, a novel endoplasmic reticulum-associated protein, facilitates TNF-α-triggered cellular apoptosis through endoplasmic reticulum-mitochondrial apoptotic pathway. J Mol Med 86, 471–484.

Lin WJ, Yang CY, Lin YC, Tsai MC, Yang CW, Tung CY, Ho PY, Kao FJ, Lin CH (2010). Phafin2 modulates the structure and function of endosomes by a Rab5-dependent mechanism. Biochem Biophys Res Commun 391, 1043–1048.

Lloyd TE, Atkinson R, Wu MN, Zhou Y, Pennetta G, Bellen HJ (2002). Hrs regulates endosome membrane invagination and tyrosine kinase receptor signaling in Drosophila. Cell 108, 261–269.

Lu H, Bilder D (2005). Endocytic control of epithelial polarity and proliferation in Drosophila. Nat Cell Biol 7, 1232–1239.

Markgraf DF, Ahnert F, Arlt H, Mari M, Peplowska K, Epp N, Griffith J, Reggiori F, Ungermann C (2009). The CORVET subunit Vps8 cooperates with the Rab5 homolog Vps21 to induce clustering of late endosomal compartments. Mol Biol Cell 20, 5276–5289.

Melnick MB, Noll E, Perrimon N (1993). The Drosophila stubarista phenotype is associated with a dosage effect of the putative ribosome-associated protein D-p40 on spineless. Genetics 135, 553–564.

Morrison HA, Dionne H, Rusten TE, Brech A, Fisher WW, Pfeiffer BD, Celniker SE, Stenmark H, Bilder D (2008). Regulation of early endosomal entry by the Drosophila tumor suppressors Rabenosyn and Vps45. Mol Biol Cell 19, 4167–4176.

Mullock BM, Bright NA, Fearon CW, Gray SR, Luzio JP (1998). Fusion of lysosomes with late endosomes produces a hybrid organelle of intermediate density and is NSF dependent. J Cell Biol 140, 591–601.

Nagano M, Hoshino D, Sakamoto T, Kawasaki N, Koshikawa N, Seiki M (2010). ZF21 protein regulates cell adhesion and motility. J Biol Chem 285, 21013–21022.

Nordmann M, Cabrera M, Perz A, Brocker C, Ostrowicz C, Engelbrecht-Vandre S, Ungermann C (2010). The Mon1-Ccz1 complex is the GEF of the late endosomal Rab7 homolog Ypt7. Curr Biol 20, 1654–1659.

Ostrowicz CW, Brocker C, Ahnert F, Nordmann M, Lachmann J, Peplowska K, Perz A, Auffarth K, Engelbrecht-Vandre S, Ungermann C (2010). Defined subunit arrangement and rab interactions are required for functionality of the HOPS tethering complex. Traffic 11, 1334–1346.

Parks AL et al. (2004). Systematic generation of high-resolution deletion coverage of the Drosophila melanogaster genome. Nat Genet 36, 288–292.

Peplowska K, Markgraf DF, Ostrowicz CW, Bange G, Ungermann C (2007). The CORVET tethering complex interacts with the yeast Rab5 homolog Vps21 and is involved in endo-lysosomal biogenesis. Dev Cell 12, 739–750.

Pieren M, Schmidt A, Mayer A (2010). The SM protein Vps33 and the t-SNARE H(abc) domain promote fusion pore opening. Nat Struct Mol Biol 17, 710–717.

Poteryaev D, Datta S, Ackema K, Zerial M, Spang A (2010). Identification of the switch in early-to-late endosome transition. Cell 141, 497–508.

Queenan AM, Ghabrial A, Schupbach T (1997). Ectopic activation of torpedo/Egfr, a Drosophila receptor tyrosine kinase, dorsalizes both the eggshell and the embryo. Development 124, 3871–3880.

Ricard CS et al. (2001). Drosophila rab GDI mutants disrupt development but have normal Rab membrane extraction. Genesis 31, 17–29.

Richardson SC, Winistorfer SC, Poupon V, Luzio JP, Piper RC (2004). Mammalian late vacuole protein sorting orthologues participate in early endosomal fusion and interact with the cytoskeleton. Mol Biol Cell 15, 1197–1210.

Rink J, Ghigo E, Kalaidzidis Y, Zerial M (2005). Rab conversion as a mechanism of progression from early to late endosomes. Cell 122, 735–749.

Rosenfeld JL, Moore RH, Zimmer KP, Alpizar-Foster E, Dai W, Zarka MN, Knoll BJ (2001). Lysosome proteins are redistributed during expression of a GTP-hydrolysis-defective rab5a. J Cell Sci 114, 4499–4508.

Rubino M, Miaczynska M, Lippe R, Zerial M (2000). Selective membrane recruitment of EEA1 suggests a role in directional transport of clathrin-coated vesicles to early endosomes. J Biol Chem 275, 3745–3748.

Sevrioukov EA, He JP, Moghrabi N, Sunio A, Kramer H (1999). A role for the *deep orange* and *carnation* eye color genes in lysosomal delivery in *Drosophila*. Mol Cell 4, 479–486.

Sisson JC, Field C, Ventura R, Royou A, Sullivan W (2000). Lava lamp, a novel peripheral Golgi protein, is required for *Drosophila melanogaster* cellularization. J Cell Biol 151, 905–918.

Sriram V, Krishnan KS, Mayor S (2003). *deep-orange* and *carnation* define distinct stages in late endosomal biogenesis in *Drosophila melanogaster*. J Cell Biol 161, 593–607.

Sun W, Yan Q, Vida TA, Bean AJ (2003). Hrs regulates early endosome fusion by inhibiting formation of an endosomal SNARE complex. J Cell Biol 162, 125–137.

Tanaka T, Nakamura A (2008). The endocytic pathway acts downstream of Oskar in *Drosophila* germ plasm assembly. Development 135, 1107–1117.

Torres VA, Mielgo A, Barila D, Anderson DH, Stupack D (2008). Caspase 8 promotes peripheral localization and activation of Rab5. J Biol Chem 283, 36280–36289.

Ullrich O, Stenmark H, Alexandrov K, Huber LA, Kaibuchi K, Sasaki T, Takai Y, Zerial M (1993). Rab GDP dissociation inhibitor as a general regulator for the membrane association of rab proteins. J Biol Chem 268, 18143–18150.

van Meer G, Voelker DR, Feigenson GW (2008). Membrane lipids: where they are and how they behave. Nat Rev Mol Cell Biol 9, 112–124.

Vanlandingham PA, Ceresa BP (2009). Rab7 regulates late endocytic trafficking downstream of multivesicular body biogenesis and cargo sequestration. J Biol Chem 284, 12110–12124.

Varnai P, Lin X, Lee SB, Tuymetova G, Bondeva T, Spat A, Rhee SG, Hajnoczky G, Balla T (2002). Inositol lipid binding and membrane localization of isolated pleckstrin homology (PH) domains. Studies on the PH domains of phospholipase C δ_1 and p130. J Biol Chem 277, 27412–27422.

Visser Smit GD, Place TL, Cole SL, Clausen KA, Vemuganti S, Zhang G, Koland JG, Lill NL (2009). Cbl controls EGFR fate by regulating early endosome fusion. Sci Signal 2, ra86.

Vitelli R, Santillo M, Lattero D, Chiariello M, Bifulco M, Bruni CB, Bucci C (1997). Role of the small GTPase Rab7 in the late endocytic pathway. J Biol Chem 272, 4391–4397.

Wegner CS, Malerod L, Pedersen NM, Progida C, Bakke O, Stenmark H, Brech A (2010). Ultrastructural characterization of giant endosomes induced by GTPase-deficient Rab5. Histochem Cell Biol 133, 41–55.

Weisz A, Basile W, Scafoglio C, Altucci L, Bresciani F, Facchiano A, Sismondi P, Cicatiello L, De Bortoli M (2004). Molecular identification of ERα-positive breast cancer cells by the expression profile of an intrinsic set of estrogen regulated genes. J Cell Physiol 200, 440–450.

Wodarz A (2008). Extraction and immunoblotting of proteins from embryos. In: Drosophila: Methods and Protocols, Vol. 420, ed. C. Dahmann, Totowa, NJ: Humana, 335–345.

Wucherpfennig T, Wilsch-Brauninger M, Gonzalez-Gaitan M (2003). Role of *Drosophila* Rab5 during endosomal trafficking at the synapse and evoked neurotransmitter release. J Cell Biol 161, 609–624.

Wurmser AE, Sato TK, Emr SD (2000). New component of the vacuolar class C-Vps complex couples nucleotide exchange on the Ypt7 GTPase to SNARE-dependent docking and fusion. J Cell Biol 151, 551–562.

Yagisawa H, Sakuma K, Paterson HF, Cheung R, Allen V, Hirata H, Watanabe Y, Hirata M, Williams RL, Katan M (1998). Replacements of single basic amino acids in the pleckstrin homology domain of phospholipase C-δ1 alter the ligand binding, phospholipase activity, and interaction with the plasma membrane. J Biol Chem 273, 417–424.

Yan Y, Denef N, Schupbach T (2009). The vacuolar proton pump, V-ATPase, is required for notch signaling and endosomal trafficking in *Drosophila*. Dev Cell 17, 387–402.

Zerial M, McBride H (2001). Rab proteins as membrane organizers. Nat Rev Mol Cell Biol 2, 107–117.